A Validation Study on the Simultaneous Quantification of Multiple Wine Aroma Compounds with Static Headspace-Gas Chromatography-Ion Mobility Spectrometry (SHS-GC-IMS)

Wenyao Zhu[1,2], Frank Benkwitz[2], Bahareh Sarmadi[1], Paul A. Kilmartin[1]

[1] Wine Science Programme, The University of Auckland, Private Bag 92019, Auckland, 1142, New Zealand

[2] Kim Crawford Winery, Constellation Brands NZ, 237 Hammerichs Road, Blenheim, 7273, New Zealand

Abstract

A new quantitative method based on static headspace–gas chromatography–ion mobility spectrometry (SHS–GC–IMS) is proposed, which enables the simultaneous quantification of multiple aroma compounds in wine. The method was first evaluated for its stability and the necessity of using internal standards as a quality control measure. The two major hurdles in applying GC-IMS in quantification studies, namely, non-linearity and multiple ion species, were also investigated using the Boltzmann function and generalized additive model (GAM) as potential solutions. Metrics characterizing the model performance, including root mean squared error, bias, limit of detection, limit of quantification, repeatability, reproducibility, and recovery were investigated. Both non-linear fitting methods, Boltzmann function and GAM, were able to return desirable analytical outcomes with an acceptable range of error. Potential pitfalls that would cause inaccurate quantification *i.e.*, effects of ethanol content and competitive ionization, were also discussed. The performance of the SHS-GC-IMS method was subsequently compared against a currently established method, namely, GC-MS, using actual wine samples. These findings provide an initial validation of a GC-IMS-based quantification method, as well as a starting point for further enhancing the analytical scope of GC-IMS.

Keywords

static headspace–gas chromatography–ion mobility spectrometry (SHS–GC–IMS), wine, method development, method validation, quantitative analysis, Boltzmann function, generalized additive model (GAM), competitive ionization

1 Introduction

Being a separation technology that has only been commercialized in recent years, gas chromatography coupled with ion mobility spectrometry (GC-IMS) has rapidly gathered attention of researchers, especially from the field of food and beverage science.[1] Multiple studies have successfully applied GC-IMS for identifying food adulteration[2-4], optimizing food processing and storage conditions[5-7], assigning food origins[8-9], differentiating food quality gradings[10-11], and detecting food spoilage[12-13]. The majority of these findings have been summarized in a review article published in 2020.[7] GC-IMS is greatly appreciated for its ability to perform true orthogonal two-dimensional analyses, which considerably enhances the analytical capacity. This feature also enables non-targeted analyses that overcomes the need of prior peak identification and indifferently processes all peak information, which has been proven immensely helpful in establishing prediction models.[10-11]

Nevertheless, it remains that the major focus of research still centers around the qualitative and semi-quantitative use of the instrument, whereas quantitative studies using GC-IMS are still quite rare. Compared to gas chromatography-mass spectrometry (GC-MS), for which well-established protocols of quantitative method development are available, consensus is still to be reached even on some fundamental aspects in quantitative GC-IMS, such as the choice of curve-fitting functions[14-16], and the inclusion of internal standards during calibration[15-17]. A brief summary of recently published research articles describing the quantitative use of GC-IMS in various matrices is presented in Table 1Error! Reference source not found.. It is apparent that considerable discrepancies exist regarding GC-IMS-based quantification. Indeed, only recently has a publication regarding the practical considerations when dedicating GC-IMS for routine analyses become available[1], and protocols for GC-IMS method development are not well defined.

Furthermore, the quantification procedures of GC-IMS differ greatly to those of GC coupled to conventional detectors, such as the flame ionization detector (FID) and mass spectrometer (MS). This can be exemplified by the more confined linear dynamic ranges in GC-IMS outputs, which render the use of non-linear functions necessary over a wider concentration range. Such phenomena could be explained by the ionization source in IMS (radioactive atmospheric pressure chemical ionization, R-APCI), in addition to the formation of high-order oligomers and heterodimers with other compounds as the target compound concentration increases, thereby resulting in the plateauing of the current ion species.[1, 18] In addition, the instrumental response of the monomeric ion species does not conform to monotonic increase. Rather, it would begin to decrease as the compound concentration continues to increase and the dimer intensity becomes stronger, as illustrated in Figure 1. It hence presents an analytical hurdle in feasibly combining the information of multiple product ions pertaining to the same compound to approach more accurate quantification. Moreover, the non-linear nature of standard curves in GC-IMS further complicates the calculation of the figures of merit that are desired in method development, such as limit of detection (LOD) and limit of quantification (LOQ).

To date, and to the best of our knowledge, no peer-reviewed article has been published in attempt to systematically discuss and provide a general solution to GC-IMS-based quantification methods. Therefore, the purpose of the current paper is to propose an initial approach to address the common hurdles during the development of quantitative methods using GC-IMS systems. Also, the possibility of utilizing multiple ion species (*e.g.*, monomer and dimer) will be discussed for further improving the method accuracy and sensitivity. As a preliminary trial, the method was used to establish calibration models for several volatile compounds commonly found in wine, as have been previously identified in our earlier study[11]. The analytical performance of this method was assessed using conventional ideas and some new tools that specifically tackle issues linked to GC-IMS.

71

2 Materials and Methods

2.1 Chemicals, reference standards and wine samples

A total of 17 compounds were calibrated in the current study, including six acetate esters (methyl acetate, propyl acetate, isobutyl acetate, isoamyl acetate, amyl acetate, hexyl acetate), seven ethyl esters (ethyl propionate, ethyl butyrate, ethyl 2-methylbutyrate, ethyl isovalerate, ethyl hexanoate, ethyl octanoate, ethyl decanoate) and four higher alcohols (isobutanol, 1-butanol, isoamyl alcohol, 1-hexanol). Analytical standards (≥98% purity) of these compounds were procured from Sigma-Aldrich (Taufkirchen, BY, Germany) and were stored in a 5 °C cool room prior to use. These compounds have been successfully identified in the wine matrix using the SHS-GC-IMS method as reported in our previous publication[11], to which interested readers are referred for a detailed discussion. The compound identification process is thus not discussed in the current study in great detail.

A simulated wine matrix was prepared to account for the major source of matrix effects in wine that affect the partition behavior of volatile compounds during the establishment of the calibration models.[19] The model solution that mimics wine matrix was first prepared by dissolving 12% *v/v* HPLC grade ethanol in Type 1 water (resistivity > 18 MΩ/cm) with pH adjusted to 3.2 by tartaric acid. The ethanol used was of HPLC grade purchased from Thermo Fisher Scientific (Auckland, New Zealand). This matrix was later used to build the calibration models of the volatile compounds.

Inevitably, wines are produced with a range of alcohol contents, which requires other ethanol levels to also be inspected during calibration. Hence, three additional model solutions of 7%, 9% and 15% *v/v* ethanol were also prepared. These were used to calculate the correction factor to be applied to the quantitative results should the wine under investigation contain a higher or lower alcohol level than 12%.

An internal standard (IS) working solution was prepared by diluting 3-octanol analytical standard in HPLC grade ethanol. For each sample analyzed using the SHS-GC-IMS instrument, an aliquot of 50 µL was spiked as a quality control. The IS working solution was prepared so that the absolute amount of 3-octanol in the spiked sample was 10–15 mg/L.

For the precision trials, vintage 2018 commercial Sauvignon Blanc wine was used. For the recovery trials, vintage 2020 commercial Sauvignon Blanc wine was used. For the method comparison trials, a selection of five Sauvignon Blanc white wines from three vintages (2018, 2019, 2020) and two red wines (2020 Tempranillo and 2019 Shiraz) were used. All white wines used in the current study were produced in New Zealand, while the Tempranillo and Shiraz wines were produced in Spain and Australia, respectively. All wines had been stored in their original packaging and away from direct sunlight at room temperature before analysis.

2.2 Construction and validation of calibration models for volatile compounds

2.2.1 Preparation of calibration dilution series using analytical standards

In order to establish the calibration models for the aforementioned volatile compounds, stock solutions of each compound were first made by dissolving one drop (accurate weights determined on a four-decimal place analytical balance) of the analytical standard into 5 mL ethanol. Serial dilutions were then made by dispensing the corresponding volumes of stock solution into the model solution to make up for the final analysis-ready volume of 5 mL. The IS working solution was spiked into each sample, followed by nitrogen purge of the headspace to protect the samples from potential oxidation while awaiting analysis. Each volatile was analyzed in their common ranges as typically found in white wines. Given the non-linear nature of the instrumental response, particular attention was paid to increase the number of calibration points, such that the curvature can be more accurately depicted. In the current

study, at least eight calibration points (excluding zero points where only pure model solution was analyzed) were tested for each volatile compound.

2.2.2 Fitting of standard curves

Since SHS-GC-IMS features a small dynamic range, a non-linear standard curve is often necessary to depict the relationship between the compound concentration and the instrument response. According to the instrument manufacturer recommendations, the Boltzmann function is useful when considering the concentration-response relationship for the dimer ion of a compound. The Boltzmann function features the following generic form:

$$y = b + \frac{a - b}{1 + \boldsymbol{e}^{\frac{\ln(x) - c}{d}}} \quad (1)$$

where a, b, c, d are constant coefficients, y = the signal intensity (volume-under-area-minimum, *a.u.*), x = analyte concentration (μg/L or mg/L). This function originated from the mathematical relationship of non-equilibrium thermodynamics and can also be used to depict ions travelling along an electric gradient.

Another method named the generalized additive model (GAM) was also used to simultaneously consider the signals of both monomer and dimer ions for predicting the compound concentration. GAM is a nonparametric method that directly reads the data without predefining a fixed mathematical expression for the concentration-response relationship. The main concept behind GAM can be expressed as:

$$g(\mathbb{E}[y|X]) = A_i\theta + f_1(x_1) + f_2(x_2) + f_3(x_3) + \cdots + f_i(x_i) + \epsilon \quad (2)$$

where $g(\mathbb{E}[y|X])$ represents the expectation of the dependent variable y from a matrix of independent variables X as modelled by the link function (identity function in the case of regression); $A_i\theta$ is the parametric terms of the independent variable; $f_i(x_i)$ is the i-th term of the independent variable modelled using spline functions; ϵ is the intercept term. According

to Hastie, Tibshirani and Friedman, a spline function is a piecewise polynomial function that is smooth in connecting knots between polynomial pieces.[20] Thus, this method utilizes a combination of basis spline functions to map the non-linear trend of calibration data points.

Alternatively, the investigated concentration range for some compounds still approximate a linear response range, in which case the linear fitting was also assessed for its characterization of the concentration-response relationship.

The goodness-of-fit of different fitting methods was evaluated using the root mean squared error (RMSE) and the systematic error (bias) as calculated using Equations 3 and 4.[21] Both metrics have the same unit as the concentration of the calibrated compound.

$$\text{RMSE} = \sqrt{\frac{\sum_{i=1}^{n}\left(c_i - c_i^{\text{reg}}\right)^2}{n}} \tag{3}$$

$$\text{bias} = \frac{\sum_{i=1}^{n}\left(c_i^{\text{reg}} - c_i\right)}{n} \tag{4}$$

2.2.3 Limit of detection (LOD) and limit of quantification (LOQ)

Given the non-linear feature of the Boltzmann function, the conventional method of estimating the LOD and LOQ using the slope of the linear standard curve is not applicable. Hence, the current study adopted the methods described by Hayashi *et al*. and González *et al*. that enable the calculation of LOD and LOQ from non-linear calibration functions.[22-23] This method considers the relative standard deviation of the back-calculated analyte concentrations (denoted as ρ_x) and the first-order derivative of the original function (denoted as D). It is mandated that $\rho_x = \left|\sigma_y / x \cdot D\right| = 30\%$ when LOD is reached and $\rho_x = 20\%$ when LOQ is reached. σ_y is the standard error of instrument response estimates. y_i and y_i^{reg} represents the actual instrument response and the predicted instrument response, respectively. In the case of Boltzmann functions:

$$D|_{\text{Boltzmann}} = \frac{(b-a)\cdot \boldsymbol{e}^{\frac{\ln(x)-c}{d}}}{d\cdot x\left(\boldsymbol{e}^{\frac{\ln(x)-c}{d}}+1\right)^2} \quad (5)$$

$$\sigma_y\big|_{\text{Boltzmann}} = \sqrt{\frac{\sum_{i=1}^{n}\left(y_i - y_i^{\text{reg}}\right)^2}{n-4}} \quad (6)$$

160 Hence, the LOD and LOQ can be calculated as follows:

$$\text{Let: } P = \left[\frac{0.3(b-a)}{d\cdot\sigma_y} - 2\right] \text{ and } Q = \left[\frac{0.2(b-a)}{d\cdot\sigma_y} - 2\right] \quad (7)$$

$$\text{LOD}|_{\text{Boltzmann}} = \boldsymbol{e}^{c}\cdot\left(\frac{P+\sqrt{P^2-4}}{2}\right)^{d} \quad (8)$$

$$\text{LOQ}|_{\text{Boltzmann}} = \boldsymbol{e}^{c}\cdot\left(\frac{Q+\sqrt{Q^2-4}}{2}\right)^{d} \quad (9)$$

161 Since the method applies universally to both linear and non-linear standard curves, it was
162 used to calculate the LOD and LOQ for all Boltzmann and linear fittings. In the case of linear
163 standard curves with the generic form of $y = kx + m$, the LOD and LOQ calculations are as
164 follows:

$$\sigma_y\big|_{\text{linear}} = \sqrt{\frac{\sum_{i=1}^{n}\left(y_i - y_i^{\text{reg}}\right)^2}{n-2}} \quad (10)$$

$$\text{LOD}|_{\text{linear}} = \frac{\sigma_y\big|_{\text{linear}}}{0.3k} \quad (11)$$

$$\text{LOQ}|_{\text{linear}} = \frac{\sigma_y\big|_{\text{linear}}}{0.2k} \quad (12)$$

165 Another method suggested by the International Union of Pure and Applied Chemistry (IUPAC)
166 was also considered.[24-25] This method calculates the LOD and LOQ as follows:

$$\text{LOD} = \overline{y} + K_D \times \sigma \quad (13)$$

$$\text{LOQ} = \overline{y} + 3 \times K_D \times \sigma \quad (14)$$

$$K_D = t(v, \alpha) \times \sqrt{1 + \frac{1}{n_B}} \quad (15)$$

In equations (13) to (15), n_B is the number of blank samples for a particular calibration and $t(v, \alpha)$ is the student *t*-statistic value of degrees of freedom (calculated as $n_B - 1$,) and confidence interval of α (set as 0.05).[24] Since this method does not involve the inspection of the original mathematical equation, it thus provides an approach to calculate LOD and LOQ in GAM applications, although in the current study it was also tested on Boltzmann- and linear-based models.

2.2.4 Repeatability and reproducibility

The repeatability and reproducibility of the SHS-GC-IMS method in terms of retention and drift times has been reported in our previous study.[11] Hence, in the current study special focus was placed on the repeatability and reproducibility of the quantification results, while employing the same data reported in the previous study. A moderately aged (50-months old at the time of analysis) Sauvignon Blanc wine was analyzed in quadruplicates per day for five days. The repeatability and reproducibility were calculated as intra- and inter-day variations, respectively.

2.2.5 Accuracy and recovery

Trueness is defined as the measurement of the deviation of a measured value to the actual value of an analyte in a sample. Therefore, this parameter demonstrates the bias in an analytical method. The lack of trueness would indicate the presence of systematic error within the method, which renders the method impractical for its intended purpose. Given the absence of certified reference materials for volatile analyses, trueness in the current validation study is expressed as the recovery rate in the spike-and-recovery trial. All spike-and-recovery tests were conducted using a vintage 2020 Marlborough Sauvignon Blanc wine,

apart from those of amyl acetate, for which a vintage 2021 Marlborough Sauvignon Blanc wine was used. The total concentration of a volatile compound in its spiked sample was controlled such that it still falls within the calibration range.

2.2.6 Examination of ethanol content effects

Ethanol has been shown to considerably alter the availability of volatiles in the headspace of wine samples as its high content in wine can suppresses the partition of other aroma compounds.[26] Thus, all aroma compounds validated in the current study were additionally tested in 7%, 9% and 15% *v/v* ethanol model solutions with their pH adjusted to 3.2. Their calculated concentrations (denoted as "apparent concentration") from these model solutions were compared with that obtained using the 12% *v/v* ethanol model solution to evaluate the deviation and calculate correction factors to compensate for the ethanol level difference.

2.2.7 Examination of competitive ionization effects

As previously highlighted by Borsdorf and Eiceman, as multiple compounds of different ionization energies (IE) or proton affinities (E_{pa}) enter the IMS ionization chamber simultaneously, competitive ionization could occur such that the compound with lower IE (or higher E_{pa}) becomes preferentially ionized, whereas other compounds are deprived of ions and are thus not eventually detected.[27] This effect was also investigated in the current study where co-elution occurred between 1-propanol and ethyl butyrate. A simulated matrix was prepared with the concentration of 1-propanol maintained at 12 mg/L in a 5 mL model solution. Ethyl butyrate was incrementally spiked into the simulated matrix from 0 to 660 µg/L to inspect the change of signal intensities in 1-propanol and ethyl butyrate peaks.

2.2.8 Method comparison between SHS-GC-IMS and HS-SPME-GC-MS

A selection of seven wines were tested using both methods. The protocol of the HS-SPME-GC-MS method was in-house developed at the University of Auckland. Readers are referred to Lyu *et al.*[28] for detailed sample pre-treatment and instrumental conditions.

2.3 Instrumentation and method parameters

Instrumentation and method details were the same as reported in a previous publication.[11] The G.A.S. FlavourSpec SHS-GC-IMS system was used in the current study (Gesellschaft für Analytische Sensorsysteme mbH, Dortmund, Germany). The instrument was fitted with a MXT-WAX polar column (30 m length × 0.53 mm internal diameter × 0.5 µm film thickness, 100% crossbond Carbowax polyethylene glycol stationary phase) purchased from RESTEK (Bellefonte, PA, USA). An autosampler (CTC Analytics AG, Zwingen, Switzerland) was also connected for the automated static headspace sample introduction on the GC column.

For sample preparation, five milliliters of each prepared sample were transferred into a 20 mL headspace vial using a micropipette, which was then purged with nitrogen and tightly crimped. Each sample vial was incubated at 40 °C for 10 minutes for equilibration, before 500 µL of the headspace gas was extracted with a heated (80 °C) syringe and injected through a heated injection port on the GC column. The GC column was set in isothermal mode at 40 °C. In GC, the carrier gas flow was first held steady at 2 mL/min for one minute, and then gradually increased to 40 mL/min at a rate of 2 mL/min^2 until 20 min. The flow was then immediately increased to 150 mL/min and held at this rate until 50 min. From 50 to 52 min, the flow rate was dropped to 2 mL/min again, before the program finished.

Following GC separation, the compounds were first ionized in the IMS ionization chamber using a tritium (^{3}H) source. The ionization was conducted under positive ion mode. Ionized volatile compounds then entered the IMS drift tube (98 mm), where an electric field (strength:

500 V/cm) was applied. The IMS device was programmed at 75 °C with a constant drift gas flow rate of 150 mL/min counter-current of the analyte ion swarm. Each IMS spectrum was acquired as the average of six scans.

Also, as a critical component of regular instrument upkeep, an intermittent 4-hour thermal cleaning was performed at the conclusion of each sample sequence and a 24-hour thermal cleaning was performed each week over the weekend, which has been shown to reduce memory effects of the GC column and ensure the consistent and desirable analytical results.

2.4 Data processing and statistical analyses

The software suite distributed with the SHS-GC-IMS instrument, LAV (Laboratory Analytical Viewer, version 2.2.1, Dortmund, Germany), was used to process the raw data acquired from each run. The LAV-quantitation module was used to obtain the signal intensities of each volatile compound as peak *volume-under-the-shape*. Microsoft Excel 2019 (Redmond, WA, USA) was used to collate raw data and perform basic calculations such as limits of detection and quantification. The programming language R (version 4.0.2, Vienna, Austria) and Python (version 3.8.3, Fredericksburg, VA, USA) was used to run ANOVA analyses, generate plots, compute the standard curves of Boltzmann function and GAM. For all *post-hoc* Tukey's HSD tests for ANOVA, the significance level was set at 5%. The error bars of all plots where they are available indicate the range of ± standard error.

3 Results and Discussion

3.1 Overall quality control of the method

As shown above in Table 1**Error! Reference source not found.**, most quantification studies did not report specifically the involvement of internal standards during method calibration or in quantitative analyses. However, ensuring the quality of semi-quantitative information obtained from SHS-GC-IMS is a crucial first step in checking for intrinsic sources of error that might lower the credibility of the final quantitative results. Hence, a method for monitoring the instrument performance was established using an internal standard spiking solution. Variations in internal standard signals could reveal the perturbations caused by a series of sources of errors, such as operator's pipetting error, autosampler injection, and GC column conditions. The internal standard was selected such that it did not interfere or react with any compounds that inherently exist in the target matrix, while also belonging to one of the same chemical categories as the target compounds of analysis.[29]

Based on these criteria, 3-octanol was selected in the current study as the internal standard and was mixed with samples in 1:100 ratio to achieve a final concentration in the sample of 10-15 mg/L. The peak for 3-octanol was well separated from those of the intrinsic volatile compounds (Supplementary Figure 1). Also, being a member of the higher alcohols group and thus sharing similar ionization behaviors, excessive fluctuations in the 3-octanol peak signal, if any, could reflect potential inaccuracy in analyzing wine volatile compounds. Two batches of internal standard solution were prepared during the current study, with concentrations of 12.6 mg/L and 14.0 mg/L, which were used to spike 240 and 139 samples in the timespan of 6 months, respectively. The second batch of IS was successively used after the first IS was depleted to cover the needs of IS dosing for all samples. A control chart was plotted for each of the two batches as shown in Figure 2 (A) and (B). The average signal intensity values of the first and the second internal standard batches were 18889±2070 and 21082±2886, with

relative standard deviations (RSD) being 11.0% and 13.7%. Hence, the stability of the method was demonstrated by possessing % RSD lower than 15%. Also, it can be seen from the control chart that in both batches, only eight points (2.1% of all samples) fell within the warning range (shown as red shaded region) and no point fell beyond the control limits, which further consolidates the suitability of the current method in volatile analyses.

By contrast, the HS-SPME-GC-MS method that was developed at the University of Auckland indicated much higher level of RSD in the 3-octanol internal standard signals during method calibration (21.8-37.5%, unpublished results). Such a difference could be explained, at least partially, by the fact the static headspace extraction in the SHS-GC-IMS instrument is a bi-phase system, where only one partition occurs between the liquid fraction of the sample and the gaseous headspace. On the other hand, when pre-concentration devices such as SPME fibers are being used, a tri-phase system is established, where partition can occur between liquid sample and the headspace, as well as between the headspace and the SPME fiber. Therefore, increased instability is introduced into the HS-SPME-GC-MS method as samples are incubated for a fixed amount of time regardless of equilibria between the three phases. Rather, in SHS-GC-IMS, it has been experimentally shown that equilibrium between liquid sample and headspace is reached after 10 minutes of incubation and agitation (see Figure 2 (C) and (D).). This phenomenon in turn indicates that stable results can be expected after headspace equilibrium is established.

In addition to analytical output monitoring, the internal standard was also used for manually adjusting the chromatograms should deviations on the retention time axis occur. The LAV software that accompanies the GC-IMS instrument allows the user to configure "area sets", *i.e.*, pre-defined boxes to accommodate peaks on the contour plot. It was quite commonly observed that misaligned chromatograms have peaks of both intrinsic compounds and the internal standard partially or entirely located outside of their corresponding boxes due to

shifts in retention times (*y* axis of the chromatogram). In manual alignments, retention time correction to relocate the misaligned IS peak back to its box could also move all other peaks back to their correction positions, which is critical for the software to correctly extract the peak signal intensities. This approach was also recommended by Jurado-Campos, Martín-Gómez, Saavedra and Arce, who reported that using internal standard as a base for plot alignment could apparently improve the homogeneity of peak positions.[1]

3.2 Selection of standard curve fitting methods

3.2.1 Hurdles in curve-fitting: non-linearity and multiple ion species

One of the most distinct features that immediately differentiate IMS from other commonly used GC detectors is its narrow linear dynamic range and the non-linear response commonly observed when a series of concentrations is used to construct a standard curve. For example, a concentration-response scatter plot of ethyl hexanoate, a common volatile found in wine, for which clear non-linear relationship was identified, is provided in Figure 3 (A). Around the lower concentrations, the concentration-signal relationship was more linear, whereas the signal became more plateaued as the concentration increased, leading to curvature across the normal concentration range of this compound in the target matrix. This effect has been widely reported for many other compounds as well.[14, 21, 30] One potential solution to circumvent this issue is dilution of the original sample so that the concentration of the target compound is lowered to reach its linear dynamic range.[31]

However, as wine is a highly complicated system consisting of multiple volatile compounds of interest, each with its own linear range and non-linear curvature, it would be exceedingly arduous to analyze even one sample with multiple dilution factors so that all volatiles would fall within their desired linear range. As a result, previous efforts have been made to use various mathematical relationships, including polynomial, logarithmic, and Boltzmann

functions, to circumvent this problem using dilutions and to directly account for the non-linear relationship.[14-15, 17] Currently, no consensus has been achieved regarding the mathematical function that best describes this curvature. In this study, the recommended mathematical model by the manufacturer: Boltzmann function, was first trialled (Figure 3 (B)), followed by the non-parametric fitting method of generalized additive model (GAM) (Figure 3 (C)), as exemplified using ethyl hexanoate.

As the complexity of fitting model increased, the fitting error decreased accordingly. The linear fitting was consistently problematic at both lower and higher concentrations. The Boltzmann fitting exhibited improvement at the lower concentration end whereas for the higher concentrations, there was still a drift away from the ideal model. The GAM fitting performed the most desirably, as no severe deviation from the ideal model was observed. This downward trend in the lack-of-fit was measured by the decreasing root mean squared error of calibration (RMSE) values (Figure 3 (D)).

Furthermore, an additional benefit of GAM compared to other fitting methods is its ability to accept multiple input variables when constructing the fitting, which becomes particularly useful when multiple ion species exist for one compound. Hence, for these compounds, the GAM method was tested both on the monomer/dimer pair and on the dimer only. These proposed methods could thus solve the problem of non-linear response behavior and multiple ion species in GC-IMS detection.

3.2.2 Comparison of the goodness-of-fit

In order to more comprehensively compare the accuracy of the different fitting methods, a compendium of the RMSE and systematic bias values of the three fitting methods for all studied compounds is presented in Table 2. The GAM fitting results were invariably better than Boltzmann and linear fittings, as demonstrated by lower RMSE values, apart from that of

ethyl decanoate where GAM performed slightly less favorably. Extremely small systematic bias figures also indicate that no severe under- or over-estimation was expected. Additional involvement of the monomer in the GAM, however, did not necessarily produce significantly improved fitting performance compared to the GAM fitting using only the dimer. This was also shown by the *p*-value of the monomer term coefficients, as only that of 1-hexanol was below 0.1. The Boltzmann function fitting, which is recommended by the instrument manufacturer, also provides a desirable alternative to GAM, despite its higher general over-estimation in the quantitative results than the GAM model. Nevertheless, such systematic bias is still acceptable considering the wide calibration range used. Overall, GAM achieved smaller RMSE values than the Boltzmann fitting, whereas the Boltzmann fitting has a stronger theoretical background as it describes the flow of ions travelling within an electric gradient. The combined use of monomers and dimers in some GAM-based models, on the other hand, only provided marginal benefits compared to their dimer-only counterparts. Therefore, both fitting methods can be considered as suitable for establishing the calibration models using the SHS-GC-IMS.

However, the GAM method is not without its problems. One of the most prominent difficulties in applying the GAM method lies in the fact that it directly reads the trend from the data per se, thereby rendering the final output greatly prone to any experimental errors from collecting the calibration data. This could result in unusual local maxima/minima in the fitted curve and thus break the monotonicity principle in the concentration-signal relationship, as exemplified by 1-butanol (see Supplementary Figure 2). Hence, visual inspection of the fitted curve needs to be exercised when GAM is being used to establish the standard curve. In this case, either the corresponding calibration concentrations may be re-conducted where experimental errors can be clearly identified, or parametric models, *i.e.*, the Boltzmann function may be used instead.

In light of the aforementioned results, it was decided that for this study, both GAM and Boltzmann function fitting would be evaluated in the subsequent figures of merit calculations. In the case of GAM being unable to produce reliable fitting curves, the Boltzmann function should be used instead as a fallback alternative.

3.3 General figures of merit of the method

3.3.1 Limit of detection (LOD) and limit of quantification (LOQ)

Using the methods described in the Materials and Methods section, the limit of detection (LOD) and limit of quantification (LOQ) were calculated for the 17 compounds studied in the simulated wine matrix.

It should be noted that the IUPAC-recommended method was not suitable for the Boltzmann-based standard curves, since sometimes the signal intensities acquired from blank samples are unable to return a valid concentration using this type of model. This is attributed to the fact that the Boltzmann features a sigmoidal curve with upper and lower asymptotes of $y = a$ and $y = b$, respectively (a and b being coefficients of the fitted Boltzmann function). Hence, any signal that falls outside the (b, a) range is not able to return a valid calculated concentration. It is not uncommon that in blank samples, the signal intensity of a given compound is lower than the coefficient b. Therefore, all LOD and LOQ values were calculated using the method proposed by Hayashi *et al*. and González *et al*. for Boltzmann function models.[22-23]

The LOD and LOQ values of the different non-linear fitting methods are collated in Table 3. Due to the different methods used to calculate the LOD and LOQ, these values tend to be higher for Boltzmann function models, which also renders them not directly comparable with those of GAM methods. Nevertheless, it could still be seen that both GAM and Boltzmann function are able to show desirable detection and quantification limits for all compounds

399 studied considering the calibration ranges applied in this study and their regular presence in
400 wines[28, 32-33], which justifies the applicability of the current method for wine aroma analyses.
401 The use of GAM on the monomer/dimer pair did improve those limits compared to GAM being
402 applied on dimer alone for some compounds, including propyl acetate, ethyl octanoate, and 1-
403 hexanol, which warrants the preferential use of GAM when a compound is only found in
404 concentrations barely above the Boltzmann fitting LOD/LOQ. This trend, however, did not
405 hold true for all compounds. Also, it could be shown from both LOD/LOQ values and the RMSE
406 values that the models with better fits (smaller RMSE) are likely to have higher
407 detection/quantification limits, which indicates compromises were made to enhance the
408 general fitting precision in exchange for the model performance at the lower end of
409 calibration.

410 *3.3.2 Method precision and accuracy*

411 The precision of quantification models was demonstrated in terms of repeatability (intra-day
412 variation) and reproducibility (inter-day variation). As can be seen from Figure 4 (A), the
413 precision values of most compounds were below 10% using either of the three quantification
414 models, which indicated desirable robustness of both the analytical and the quantitative
415 calculation methods.

416 It was also immediately recognizable, however, that the precision of ethyl decanoate was
417 notably worse than that of other compounds. It was revealed by further investigation that for
418 each day, the ethyl decanoate signal in the first analyzed sample was consistently lower than
419 that in subsequent samples. Such a phenomenon could be due to the fact that the instrument
420 was always thermally cleaned at 80 °C at the end of each day, which was essential to minimize
421 retention time and drift time variations as the instrument operates under isothermal GC
422 mode.[11] The cleaning process also clears the column from residual apolar compounds that
423 were unable to detach from the column before the end of each run, which, conversely, was not

executed between samples and could thus increases the stationary phase hydrophobicity. A close inspection of the physiochemical properties of ethyl decanoate highlighted that its *log P* value is in the range 3.61-4.43, which infers a stronger tendency to interact with the hydrophobic phase.[34] Therefore, ethyl decanoate signals were less pronounced in the first sample of each day. This finding also showed the need to treat the quantification results of ethyl decanoate with care should the compound be detected in the first analyzed sample after the instrument undergoes thermal cleaning.

The accuracy of quantification was expressed in terms of the recovery of compounds in spiked samples, as collated in Figure 4 (B). Most compounds were able to receive a recovery value in the range of 60-120% with an average of 74.7%, which indicated an acceptable level of method accuracy. Ethyl propionate and isoamyl alcohol, on the other hand, returned unsatisfactory recovery rates below 60%. Hence, these two compounds were shown unsuitable to be quantified based on the current method.

Additionally, it must also be pointed out that real wine samples contain non-volatile components that have been reported to retain volatile compounds and lower their presence into the headspace, such as polyphenols and polysaccharides.[35-36] Since a simulated matrix was used in the current study, the volatiles in the calibration samples were more likely to be released from the liquid fraction compared to those in real wine samples, which could explain the relatively low recoveries. In order to compensate for the matrix effects, the quantification results of volatiles should be corrected for their respective recovery values, according to the recommendations by Thompson *et al.*, in that no single generally received protocol is available for aroma analyses and thus only recovery-corrected results are meaningful for mutual comparison with those obtained from other methods.[37]

For the majority of studied compounds, the three fitting methods achieved similar results. However, a considerable discrepancy in the recovery rates was observed for isobutyl acetate

and isoamyl acetate, ethyl isovalerate, and ethyl 2-methylbutyrate. Hence, quantification results from all of Boltzmann, GAM (D) and GAM (M,D) (if available) should be reported simultaneously, as no single method manifested distinctive superiority over others. Also, future endeavors need to be devoted to identifying the long-term applicability of these fitting methods by testing them on further matrices and conducting additional calibrations for the compounds of interest.

3.4 Influence of varying ethanol levels

One major difference between established methods for aroma analysis such as headspace-solid phase microextraction-gas chromatography-mass spectrometry (HS-SPME-GC-MS) and the currently proposed method lies in that a pre-concentration step is refrained in SHS-GC-IMS, owing to the high sensitivity of the ion mobility spectrometry. This, on the other hand, highlights the importance to examine the effects of any matrix components that either enhance or suppress the partition behavior of volatile compounds. Multiple studies have previously reported that the content of ethanol profoundly impacts major aroma compounds in alcoholic beverages in that a higher ethanol concentration can likely lower their partition abilities.[26, 38-39] In the static headspace method, according to Kolb, the amount of a given volatile compound releasable into the headspace is solely governed by the partition coefficient of the volatile, and the phase ratio between the volumes of liquid and the headspace.[40] In comparison, the application of the HS-SPME-GC-MS method usually involves the addition of salt, which enhances the overall ionic strength in the sample to override the original partition behavior of volatile compounds and coerce their distribution from the liquid into the headspace phase.[41-43] The “salting-out” phenomenon therefore renders the detection of volatiles using such method less influenced by matrix effects.

As the SHS-GC-IMS method essentially establishes a relationship between the instrument signal, which is induced by the volatile compound dispersed into the headspace, and the

concentration of compound in the liquid sample, significant perturbations in the partitioning of volatiles would hence result in under- or over-estimation of their real concentrations, when the quantification model is applied as is without corresponding corrections.

In the current study, three extra ethanol levels (7%, 9%, 15% *v/v*) to cover the common range of ethanol contents in wines were also tested, in addition to the 12% *v/v* ethanol level in which the calibration was constructed, in order to delineate the effects of varying ethanol levels on the SHS-GC-IMS quantification results. As shown in Figure 5, a linear relationship can be found between the calculated concentration of volatile compounds from the original calibration model, and the ethanol content. Such linearity holds, as evidenced by the respective coefficients of determination (R^2), across all volatiles investigated in this study, although different compounds demonstrate different extent of susceptibility towards varying ethanol levels. Also, the correction factors applicable in both GAM and Boltzmann models do not differ greatly, which again demonstrates the coherence of these calibration models. The raw results prior to correction invariably indicate an over-estimation of the actual volatile concentrations for low-alcohol wines and an under-estimation for high-alcohol wines, which is consistent with previous findings that the partition of volatile compounds is suppressed as the ethanol content increases in alcoholic beverages.[26]

A compendium of all correction factors to be applied to the calculated concentration of individual aroma compounds with respect to common ethanol contents are listed in Table 4. Therefore, users of the SHS-GC-IMS are advised to be careful with ethanol content of their samples and apply these factors where necessary.

3.5 Competitive ionization effects in co-eluting compounds

One of the characteristics that profoundly interferes with the analytical results of IMS-based methods is the competitive ionization between compounds of different ionization energies

498 and proton affinities.[27] This issue has resulted in the tandem use of GC pre-fractionation
499 before the IMS detector to improve the analytical output.[44]

500 One issue with competitive ionization was observed in the current study between 1-propanol
501 and ethyl butyrate. This effect is seen in the co-evolution curves between a fixed
502 concentration of 1-propanol and varying concentrations of ethyl butyrate (see Figure 6 (A)).
503 As the addition concentration of ethyl butyrate increased from 0 to 679.8 µg/L, the signal
504 intensities of both ion species of 1-propanol dropped significantly by 38.9% and 60.6%,
505 respectively, although this concentration of 1-propanol was maintained at 16.3 mg/L
506 throughout the experiment. A closer inspection of the raw chromatogram revealed that the
507 peaks for the two compounds overlap at a retention time of ~300 s, which indicates their
508 simultaneous presence in the IMS ionization chamber (see Figure 6 (B)). Visual examination
509 of signal peak chromatograms has also showed clear decline in 1-propanol monomer and
510 dimer signal intensities as the ethyl butyrate peak increased (see Figure 6 (C)).

511 Such behavior could be explained by different proton affinities (E_{pa}) of the two compounds.
512 The E_{pa} of 1-propanol was reported as 786.5 kJ mol^{-1}.[45] Although no experimental data is
513 available for the E_{pa} of ethyl butyrate, it could be reasonably inferred as being > 833.7–835.7
514 kJ mol^{-1}, *i.e.*, higher than the E_{pa} of ethyl acetate.[45-46] Hence, the higher proton affinity of ethyl
515 butyrate would result in its preferential ionization while suppressing that of 1-propanol,
516 when the two compounds are simultaneously subject to chemical ionization. However, as the
517 quantitative calibration process was conducted individually for each compound, the
518 calibration model would fail to correctly account for such interaction between ion and lead to
519 the general underestimation of 1-propanol. As a result, 1-propanol quantification was not
520 achieved using the current experimental setup. The competitive ionization phenomenon
521 needs to be carefully considered and possibly mitigated by switching to GC columns with

narrower inner widths in the scenario of co-elution for future calibration work using GC-IMS, to ascertain the validity of calibration models.

3.6 Comparative analyses between SHS-GC-IMS and HS-SPME-GC-MS

A comparative study was also conducted in order to delineate the discrepancies between the proposed SHS-GC-IMS method and the currently available HS-SPME-GC-MS method at the University of Auckland. It should be noted that all quantitative results obtained from HS-SPME-GC-MS method were also corrected for recoveries.

Firstly, the validation metrics for the HS-SPME-GC-MS methods were collated and are presented in Table 5. It can be observed that LOD and LOQ are generally higher for the HS-SPME-GC-MS method as opposed to SHS-GC-IMS, indicating the lower sensitivity of HS-SPME-GC-MS, whereas neither method shows considerable superiority in other metrics.

A selection of five Sauvignon Blanc white wines of three vintages (2018, 2019, 2020) and two red wines (2020 Tempranillo and 2019 Shiraz) were tested using both methods to compare their performances following the procedures recommended by Ungerer and Prerorius, and Bland and Altman.[47-49] Scatter plots and linear fittings were generated to investigate the correlation and the systematic bias, if any, between the quantitative results obtained using the two methods. It can be seen from the examples provided in Figure 7 (A) and (C) and the details in Table 6 that most compounds showed good correlation as indicated by the R^2 (> 0.87), apart from ethyl decanoate (R^2 = 0.7440) and ethyl isobutyrate (R^2 = 0.7368). The lower correlation for these two compounds could be explained by their high LOD and LOQ values of in both methods, and that the actual concentrations of these compounds in the analyzed wines were very close to the quantification limits. The systematic biases, on the other hand, can be invariably observed for all compounds as their slopes of correlation deviate from 1, which

demonstrates the need to firstly correct for such differences should the results need to be directly compared.

The Bland-Altman plots were then constructed, which aimed to show the inherent differences of the two methods. Again, two examples are provided in Figure 7 (B) and (D) and further details are presented in Table 6. Such plots calculate the mean difference between the quantification results of both methods after the compensation for systematic bias, as well as the upper/lower limits of agreement (LOA). The LOA is calculated as $\text{LOA} = \text{mean} \pm 1.96 \times s$, where s is the standard deviation of all differences. The 95% confidence intervals of the mean and LOA are calculated as the following:

$$95\%\ \text{CI mean} = \text{mean} \pm t(v, \alpha) \times \sqrt{\frac{s^2}{n}} \tag{16}$$

$$95\%\ \text{CI LOA} = \text{LOA} \pm t(v, \alpha) \times \sqrt{\frac{3s^2}{n}} \tag{17}$$

In equations (16) and (17) , n is the total number of measurements obtained from both SHS-GC-IMS and HS-SPME-GC-MS, and $t(v, \alpha)$ is the student t-statistic of v degrees of freedom (calculated as $n - 1$) and confidence interval of α (set as 0.05). The dispersion of data points on the Bland-Altman plots for all compounds, as, with the two examples given in Figure 7 (B) and (D), indicates only a small number of measurements (maximum 3 out of 42) were positioned out of the LOA boundaries, which explains the absence of inherent disagreement between the two methods aside from the systematic bias.

Since neither method has undertaken proficiency tests or been verified using reference materials, it is therefore inappropriate to name either one as a “reference method”. This comparative study has nonetheless indicated overall desirable correlations between the two methods, albeit the ubiquitous systematic biases. When the systematic bias is corrected, then the two methods did not show considerable inherent differences, as evidenced by the dispersion of data points on the Bland-Altman plots and the limits of agreement. However,

567 such a comparison between two instrumental methods in wine aroma analyses is rarely
568 presented in literature, still less the comparison involving SHS-GC-IMS. The question of
569 whether such systematic differences between two methods will indeed be dependent of the
570 desired level of accuracy that is dictated by practical needs. Definitive conclusions on the
571 accuracy of these two methods can only be drawn when reference materials are to be
572 analyzed. Nevertheless, as the SHS-GC-IMS method offers several advantages such as low
573 running cost and ease of sample handling, it then also incentivizes the user to achieve the best
574 compromise in costs and efforts of aroma analyses.

575 The current study presented an initial approach to establish the great potential of using GC-
576 IMS-based systems for the quantitative analysis of volatile compounds, using wine as an
577 exemplary matrix. Advantages of this method include superior stability and the ease of
578 sample preparation and instrument maintenance. A few hurdles such as the inevitable non-
579 linearity and occurrence of multiple ion species were tackled using non-linear the Boltzmann
580 fitting function and non-parametric generalized additive model (GAM). Metrics including the
581 goodness-of-fit, limit of detection, limit of quantification, repeatability, reproducibility, and
582 recovery were carefully evaluated. All of the fitting methods were able to return desirable
583 outcomes, while no single method demonstrated apparent superiority over others. The
584 comparison between the SHS-GC-IMS method and a currently established HS-SPME-GC-MS
585 method indicated desirable correlation and coherent method precisions in analyzing real
586 wine samples. Additionally, problems such as the effects of varying ethanol contents in wine
587 and the competitive ionization need to be promptly identified and mitigated to ensure
588 accurate analytical results.

589 The quantitative capability of GC-IMS shows that it can be employed in addition to its most
590 common use as a simple screening method. This approach offers an alternative to expensive
591 counterparts such as GC-MS, should the absolute concentration of compounds be needed. In

commercial winery laboratories, for instance, the instrument with the developed quantitative method could be integrated into the existing routine quality control workflow to provide valuable extra information. Future improvement of GC-IMS quantification could involve validation of the optimal fitting method and the optimization of the elution program to avoid co-elution of compounds to further expand the efficacy of GC-IMS-based quantification.

Acknowledgements

The authors would like to express sincere gratitude towards Constellation Brands, NZ, who kindly supplied us with all the wine samples used in the current study. They would also like to thankfully acknowledge Callaghan Innovation for the financial support (contract number: CONB1801).

Conflict of Interest

The authors declare no competing financial interest.

Supporting Information

This material is available free of charge via the Internet at http://pubs.acs.org.

- Figure S1 Position of the 3-octanol peak on the SHS-GC-IMS chromatogram of a wine sample.
- Figure S2. The GAM fitting curve of 1-Butanol when both monomer and dimer ions were considered.

References

1. Jurado-Campos, N.; Martín-Gómez, A.; Saavedra, D.; Arce, L., Usage considerations for headspace-gas chromatography-ion mobility spectrometry as a suitable technique for qualitative analysis in a routine lab. *J. Chromatogr. A* **2021,** *1640*, 461937.

2. Arroyo-Manzanares, N.; Martín-Gómez, A.; Jurado-Campos, N.; Garrido-Delgado, R.; Arce, C.; Arce, L., Target vs spectral fingerprint data analysis of Iberian ham samples for avoiding labelling fraud using headspace - gas chromatography-ion mobility spectrometry. *Food Chem.* **2018,** *246*, 65-73.

3. Chen, T.; Chen, X.; Lu, D.; Chen, B., Detection of Adulteration in Canola Oil by Using GC-IMS and Chemometric Analysis. *Int. J. Anal. Chem.* **2018,** *2018*, 3160265.

4. Gerhardt, N.; Birkenmeier, M.; Schwolow, S.; Rohn, S.; Weller, P., Volatile-Compound Fingerprinting by Headspace-Gas-Chromatography Ion-Mobility Spectrometry (HS-GC-IMS) as a Benchtop Alternative to (1)H NMR Profiling for Assessment of the Authenticity of Honey. *Anal. Chem.* **2018,** *90* (3), 1777-1785.

5. Ge, S.; Chen, Y.; Ding, S.; Zhou, H.; Jiang, L.; Yi, Y.; Deng, F.; Wang, R., Changes in volatile flavor compounds of peppers during hot air drying process based on headspace-gas chromatography-ion mobility spectrometry (HS-GC-IMS). *J. Sci. Food Agric.* **2020,** *100* (7), 3087-3098.

6. Li, H.; Jiang, D.; Liu, W.; Yang, Y.; Zhang, Y.; Jin, C.; Sun, S., Comparison of fermentation behaviors and properties of raspberry wines by spontaneous and controlled alcoholic fermentations. *Food Res. Int.* **2020,** *128*, 108801.

7. Li, X.; Wang, K.; Yang, R.; Dong, Y.; Lin, S., Mechanism of aroma compounds changes from sea cucumber peptide powders (SCPPs) under different storage conditions. *Food Res. Int.* **2020,** *128*, 108757.

8. Gerhardt, N.; Birkenmeier, M.; Sanders, D.; Rohn, S.; Weller, P., Resolution-optimized headspace gas chromatography-ion mobility spectrometry (HS-GC-IMS) for non-targeted olive oil profiling. *Anal. Bioanal. Chem.* **2017,** *409* (16), 3933-3942.

9. Martín-Gómez, A.; Arroyo-Manzanares, N.; Rodríguez-Estévez, V.; Arce, L., Use of a non-destructive sampling method for characterization of Iberian cured ham breed and feeding regime using GC-IMS. *Meat Sci.* **2019,** *152*, 146-154.

10. Gerhardt, N.; Schwolow, S.; Rohn, S.; Pérez-Cacho, P. R.; Galán-Soldevilla, H.; Arce, L.; Weller, P., Quality assessment of olive oils based on temperature-ramped HS-GC-IMS and sensory evaluation: Comparison of different processing approaches by LDA, kNN, and SVM. *Food Chem.* **2019,** *278*, 720-728.

11. Zhu, W.; Benkwitz, F.; Kilmartin, P. A., Volatile-Based Prediction of Sauvignon Blanc Quality Gradings with Static Headspace-Gas Chromatography-Ion Mobility Spectrometry (SHS-GC-IMS) and Interpretable Machine Learning Techniques. *J. Agric. Food Chem.* **2021,** *69* (10), 3255-3265.

643 12. Liu, J.; Liu, M.; Liu, Y.; Jia, M.; Wang, S.; Kang, X.; Sun, H.; Strappe, P.; Zhou, Z., Moisture content is a key
644 factor responsible for inducing rice yellowing. *J. Cereal Sci.* **2020,** *94*.

645 13. Gu, S.; Chen, W.; Wang, Z.; Wang, J., Rapid determination of potential aflatoxigenic fungi contamination
646 on peanut kernels during storage by data fusion of HS-GC-IMS and fluorescence spectroscopy. *Postharvest Biol.*
647 *Technol.* **2021,** *171*, 111361.

648 14. del Mar Contreras, M.; Aparicio, L.; Arce, L., Usefulness of GC-IMS for rapid quantitative analysis without
649 sample treatment: Focus on ethanol, one of the potential classification markers of olive oils. *LWT* **2020,** *120*,
650 108897.

651 15. Pu, D.; Duan, W.; Huang, Y.; Zhang, Y.; Sun, B.; Ren, F.; Zhang, H.; Chen, H.; He, J.; Tang, Y., Characterization
652 of the key odorants contributing to retronasal olfaction during bread consumption. *Food Chem.* **2020,** *318*,
653 126520.

654 16. Thomas, C. F.; Zeh, E.; Dörfel, S.; Zhang, Y.; Hinrichs, J., Studying dynamic aroma release by headspace-
655 solid phase microextraction-gas chromatography-ion mobility spectrometry (HS-SPME-GC-IMS): method
656 optimization, validation, and application. *Anal. Bioanal. Chem.* **2021,** *413* (9), 2577-2586.

657 17. Budzyńska, E.; Sielemann, S.; Puton, J.; Surminski, A. L. R. M., Analysis of e-liquids for electronic
658 cigarettes using GC-IMS/MS with headspace sampling. *Talanta* **2020,** *209*, 120594.

659 18. Kwantwi-Barima, P.; Hogan, C. J., Jr.; Clowers, B. H., Deducing Proton-Bound Heterodimer Association
660 Energies from Shifts in Ion Mobility Arrival Time Distributions. *J. Phys. Chem. A* **2019,** *123* (13), 2957-2965.

661 19. Ferreira, V.; Herrero, P.; Zapata, J.; Escudero, A., Coping with matrix effects in headspace solid phase
662 microextraction gas chromatography using multivariate calibration strategies. *J. Chromatogr. A* **2015,** *1407*, 30-
663 41.

664 20. Hastie, T.; Tibshirani, R.; Friedman, J., Basis Expansions and Regularization. In *The Elements of Statistical*
665 *Learning*, 2009; pp 139-189.

666 21. Brendel, R.; Schwolow, S.; Rohn, S.; Weller, P., Comparison of PLSR, MCR-ALS and Kernel-PLSR for the
667 quantification of allergenic fragrance compounds in complex cosmetic products based on nonlinear 2D GC-IMS
668 data. *Chemom. Intell. Lab. Syst.* **2020,** *205*, 104128.

669 22. González, O.; Blanco, M. E.; Iriarte, G.; Bartolomé, L.; Maguregui, M. I.; Alonso, R. M., Bioanalytical
670 chromatographic method validation according to current regulations, with a special focus on the non-well
671 defined parameters limit of quantification, robustness and matrix effect. *J. Chromatogr. A* **2014,** *1353*, 10-27.

672 23. Hayashi, Y.; Matsuda, R.; Ito, K.; Nishimura, W.; Imai, K.; Maeda, M., Detection Limit Estimated from Slope
673 of Calibration Curve: An Application to Competitive ELISA. *Anal. Sci.* **2005,** *21* (2), 167-169.

674 24. Mocak, J.; Bond, A. M.; Mitchell, S.; Scollary, G., A statistical overview of standard (IUPAC and ACS) and
675 new procedures for determining the limits of detection and quantification: Application to voltammetric and
676 stripping techniques. *Pure Appl. Chem.* **1997,** *69* (2), 297-328.

677 25. Karpas, Z.; Guamán, A. V.; Calvo, D.; Pardo, A.; Marco, S., The potential of ion mobility spectrometry (IMS)
678 for detection of 2,4,6-trichloroanisole (2,4,6-TCA) in wine. *Talanta* **2012,** *93*, 200-205.

679 26. Robinson, A. L.; Ebeler, S. E.; Heymann, H.; Boss, P. K.; Solomon, P. S.; Trengove, R. D., Interactions
680 between wine volatile compounds and grape and wine matrix components influence aroma compound
681 headspace partitioning. *J. Agric. Food Chem.* **2009,** *57* (21), 10313-10322.

682 27. Borsdorf, H.; Eiceman, G. A., Ion Mobility Spectrometry: Principles and Applications. *Appl. Spectrosc. Rev.*
683 **2006,** *41* (4), 323-375.

684 28. Lyu, X.; Araújo, L. D.; Quek, S.-Y.; Kilmartin, P. A., Effects of Antioxidant and Elemental Sulfur Additions at
685 Crushing on Aroma Profiles of Pinot Gris, Chardonnay and Sauvignon Blanc Wines. *Food Chem.* **2021,** *346*,
686 128914.

687 29. Wang, M.; Wang, C.; Han, X., Selection of internal standards for accurate quantification of complex lipid
688 species in biological extracts by electrospray ionization mass spectrometry-What, how and why? *Mass Spectrom.*
689 *Rev.* **2017,** *36* (6), 693-714.

690 30. Denawaka, C. J.; Fowlis, I. A.; Dean, J. R., Evaluation and application of static headspace-multicapillary
691 column-gas chromatography-ion mobility spectrometry for complex sample analysis. *J. Chromatogr. A* **2014,**
692 *1338*, 136-148.

693 31. Márquez-Sillero, I.; Aguilera-Herrador, E.; Cárdenas, S.; Valcárcel, M., Determination of 2,4,6-
694 tricholoroanisole in water and wine samples by ionic liquid-based single-drop microextraction and ion mobility
695 spectrometry. *Anal. Chim. Acta* **2011,** *702* (2), 199-204.

696 32. Antalick, G.; Perello, M.; De Revel, G., Esters in Wines: New Insight through the Establishment of a
697 Database of French Wines. *Am. J. Enol. Vitic.* **2014,** *65* (3), 293-304.

698 33. de-la-Fuente-Blanco, A.; Sáenz-Navajas, M. P.; Ferreira, V., On the effects of higher alcohols on red wine
699 aroma. *Food Chem.* **2016,** *210*, 107-114.

700 34. Souza, E. S.; Zaramello, L.; Kuhnen, C. A.; S., J. B. d.; Yunes, R. A.; Heinzen, V. E. F., Estimating the
701 octanol/water partition coefficient for aliphatic organic compounds using semi-empirical electrotopological
702 index. *Int. J. Mol. Sci.* **2011,** *12* (10), 7250-7264.

703 35. Lyu, J.; Chen, S.; Nie, Y.; Xu, Y.; Tang, K., Aroma release during wine consumption: Factors and analytical
704 approaches. *Food Chem.* **2021,** *346*, 128957.

705 36. Rodríguez-Bencomo, J. J.; Muñoz-González, C.; Andújar-Ortiz, I.; Martín-Álvarez, P. J.; Moreno-Arribas, M.
706 V.; Pozo-Bayón, M. Á., Assessment of the effect of the non-volatile wine matrix on the volatility of typical wine

aroma compounds by headspace solid phase microextraction/gas chromatography analysis. *J. Sci. Food Agric.* **2011,** *91* (13), 2484-2494.

37. Thompson, M.; Ellison, S. L. R.; Fajgelj, A.; Willetts, P.; Wood, R., Harmonized guidelines for the use of recovery information in analytical measurement. *Pure Appl. Chem.* **1999,** *71* (2), 337-348.

38. Muñoz-González, C.; Martín-Álvarez, P. J.; Moreno-Arribas, M. V.; Pozo-Bayón, M. Á., Impact of the nonvolatile wine matrix composition on the in vivo aroma release from wines. *J. Agric. Food Chem.* **2014,** *62* (1), 66-73.

39. Pham, D.-T.; Stockdale, V. J.; Jeffery, D. W.; Tuke, J.; Wilkinson, K. L., Investigating Alcohol Sweetspot Phenomena in Reduced Alcohol Red Wines. *Foods* **2019,** *8* (10), 491.

40. Kolb, B., Headspace Gas Chromatography. In *Encyclopedia of Separation Science*, 2000; pp 489-496.

41. Arcari, S. G.; Caliari, V.; Sganzerla, M.; Godoy, H. T., Volatile composition of Merlot red wine and its contribution to the aroma: optimization and validation of analytical method. *Talanta* **2017,** *174*, 752-766.

42. Azzi-Achkouty, S.; Estephan, N.; Ouaini, N.; Rutledge, D. N., Headspace solid-phase microextraction for wine volatile analysis. *Crit. Rev. Food Sci. Nutr.* **2017,** *57* (10), 2009-2020.

43. Cai, L.; Rice, S.; Koziel, J.; Dharmadhikari, M., Development of an Automated Method for Selected Aromas of Red Wines from Cold-Hardy Grapes Using Solid-Phase Microextraction and Gas Chromatography-Mass Spectrometry-Olfactometry. *Separations* **2017,** *4* (3), 24.

44. Vautz, W.; Franzke, J.; Zampolli, S.; Elmi, I.; Liedtke, S., On the potential of ion mobility spectrometry coupled to GC pre-separation - A tutorial. *Anal. Chim. Acta* **2018,** *1024*, 52-64.

45. Hunter, E. P. L.; Lias, S. G., Evaluated Gas Phase Basicities and Proton Affinities of Molecules: An Update. *J. Phys. Chem. Ref. Data* **1998,** *27* (3), 413-656.

46. Holmes, J. L.; van Huizen, N. A.; Burgers, P. C., Proton affinities and ion enthalpies. *Eur. J. Mass Spectrom.* **2017,** *23* (6), 341-350.

47. Bland, J. M.; Altman, D. G., Statistical methods for assessing agreement between two methods of clinical measurement. *Lancet* **1986,** *327* (8476), 307-310.

48. Bland, J. M.; Altman, D. G., Measuring agreement in method comparison studies. *Stat. Methods Med. Res.* **1999,** *8* (2), 135-160.

49. Ungerer, J. P. J.; Pretorius, C. J., Method comparison - a practical approach based on error identification. *Clin. Chem. Lab. Med.* **2017,** *56* (1), 1-4.

50. Raza, A.; Song, H.; Begum, N.; Raza, J.; Iftikhar, M.; Li, P.; Li, K., Direct Classification of Volatile Organic Compounds in Heat-Treated Glutathione-Enriched Yeast Extract by Headspace-Gas Chromatography-Ion Mobility Spectrometry (HS-GC-IMS). *Food Anal. Methods* **2020,** *13* (12), 2279-2289.

739 51. Jin, Y.; Shu, N.; Xie, S.; Cao, W.; Xiao, J.; Zhang, B.; Lu, W., Comparison of 'Beibinghong' dry red wines from
740 six producing areas based on volatile compounds analysis, mineral content analysis, and sensory evaluation
741 analysis. *Eur. Food Res. Technol.* **2021,** *247* (6), 1461-1475.

742 52. Speckbacher, V.; Zeilinger, S.; Zimmermann, S.; Mayhew, C. A.; Wiesenhofer, H.; Ruzsanyi, V., Monitoring
743 the volatile language of fungi using gas chromatography-ion mobility spectrometry. *Anal. Bioanal. Chem.* **2021,**
744 *413* (11), 3055-3067.

745

Table 1. Summary of recent research publications on applying GC-IMS in quantitative analyses of volatile compounds.

Matrix of interest	Quantification method	Figures of merit (e.g., LOD, LOQ, recovery)	Number of quantified compounds	Use of internal standard	Ref.
yeast extract	relative semi-quantification adjusted against internal standard concentration	none reported	52	yes	50
white bread	dilution series of external standards without matrix and fitted to Boltzmann and linear functions	goodness-of-fit; linear range	44	not reported	15
heat- and acid-modified bovine dairy mix	dilution series of external standards in the original matrix and fitted to linear function	LOD; LOQ; recovery; precision	11	not reported	16
red wine (made from *Vitis amurensis*)	relative semi-quantification adjusted against internal standard concentration	none reported	46	yes	51
sunflower oil	dilution series of external standards in the original matrix data processed with spectrum unfolding coupled with multivariate regression methods: MCR-ALS and (*k*-) PLSR	standard error of prediction (SEP); relative percentage error of prediction (RE)	2	not reported	21
pathogenic fungi	dilution series of nebulized mix of external standards without matrix and fitted to linear function	LOD; LOQ; linear dynamic range; precision	14	not reported	52
olive oil	dilution series of the external standard (ethanol) in simulated matrix and fitted to linear and logarithmic functions	LOD; LOQ; precision	1	not reported	14
Natural and artificial fabrics	dilution series of external standards in simulated matrix and fitted to linear and polynomial functions	LOD; LOQ; goodness-of-fit; linear dynamic range	30		30
electronic cigarette liquid	dilution series of external standards in methanol/water	LOD; LOQ; calibration range; goodness-of-fit	8	not reported	17

matrix and fitted to linear and
polynomial functions

746

Table 2. RMSE and systematic bias figures of GAM, Boltzmann function fitting and linear fitting on the calibration points of the volatile compounds calibrated in simulated wine matrix. Units for the reported figures are µg/L unless otherwise specified.

Compound	Calibration range	GAM (M,D) [a]		GAM (D) [b]		Boltzmann function		Linear function	
		RMSE	Bias	RMSE	Bias	RMSE	Bias	RMSE	Bias
Methyl acetate	0 – 687.8	—	—	10.8	*i.f.t.m.* [c]	12.2	0.5	62.4	*i.f.t.m.*
Propyl acetate	0 – 694.4	10.3	*i.f.t.m.*	10.6	*i.f.t.m.*	11.7	0.2	169.7	154.0
Isobutyl acetate	0 – 712.8	5.0	*i.f.t.m.*	5.3	*i.f.t.m.*	7.4	0.3	101.1	*i.f.t.m.*
Isoamyl acetate	0 – 6732.0	—	—	59.7	*i.f.t.m.*	167.8	12.9	1062.1	*i.f.t.m.*
Amyl acetate	0 – 807.8	—	—	16.9	*i.f.t.m.*	30.3	1.7	93.1	0
Hexyl acetate	0 – 1544.4	—	—	17.5	*i.f.t.m.*	43.8	4.6	184.0	*i.f.t.m.*
Ethyl isobutyrate	0 – 533.9	—	—	17.0	*i.f.t.m.*	19.9	12.1	88.1	*i.f.t.m.*
Ethyl isovalerate	0 – 618.1	—	—	3.2	*i.f.t.m.*	9.63	0.9	79.5	*i.f.t.m.*
Ethyl 2-methylbutyrate	0 – 620.4	—	—	3.3	*i.f.t.m.*	11.2	1.4	90.8	0
Ethyl propionate	0 – 495.0	15.3	*i.f.t.m.*	15.0	*i.f.t.m.*	19.5	0.61	64.7	*i.f.t.m.*
Ethyl butyrate	0 – 1029.6	—	—	14.6	*i.f.t.m.*	19.7	0.2	159.6	*i.f.t.m.*
Ethyl hexanoate	0 – 2398.0	—	—	31.6	*i.f.t.m.*	183.0	23.9	385.0	*i.f.t.m.*

Ethyl octanoate	0 – 3009.6	45.0	*i.f.t.m.*	44.5	*i.f.t.m.*	51.1	1.33	140.1	*i.f.t.m.*
Ethyl decanoate	0 – 1039.5	—	—	19.3	*i.f.t.m.*	18.9	0.4	19.3	*i.f.t.m.*
Isobutanol [c]	0 – 167.8	0.8	*i.f.t.m.*	0.9	*i.f.t.m.*	3.7	0.6	25.4	*i.f.t.m.*
1-Butanol [c]	0 – 62.0		*GAM defied monotonicity*			5.0	0.3	12.9	*i.f.t.m.*
Isoamyl alcohol [c]	0 – 329.7	1.2	*i.f.t.m.*	2.6	*i.f.t.m.*	26.5	4.6	64.6	0
1-Hexanol	0 – 3626.8	16.1	*i.f.t.m.*	31.0	*i.f.t.m.*	80.7	1.0	80.0	*i.f.t.m.*

a) The GAM method using both monomer and dimer signals;

b) The GAM method using the dimer signal only;

c) *i.f.t.m* represents infinitesimally small, *i.e.*, below 1×10^{-5};

d) Units for the metrics related to these compounds are mg/L.

Table 3. LOD and LOQ figures of GAM and Boltzmann function fitting on the calibration points of the volatile compounds calibrated in simulated wine matrix. Units for the reported figures are µg/L unless otherwise specified.

Compound	Calibration range	GAM (M,D) [a]		GAM (D) [b]		Boltzmann function	
		LOD	LOQ	LOD	LOQ	LOD	LOQ
Methyl acetate	0 – 687.8	—	—	13.3	37.9	13.9	22.8
Propyl acetate	0 – 694.4	3.4	8.3	3.3	10.9	6.5	10.6
Isobutyl acetate	0 – 712.8	3.3	10.0	0.04	0.3	4.7	9.6
Isoamyl acetate	0 – 6732.0	—	—	1.6	2.4	26.1	70.2
Amyl acetate	0 – 807.8	—	—	2.1	3.6	12.0	17.3
Hexyl acetate	0 – 1544.4	—	—	6.9	18.8	40.2	64.6
Ethyl isobutyrate	0 – 533.9	—	—	0.4	1.1	15.8	58.5
Ethyl isovalerate	0 – 618.1	—	—	0.3	1.1	5.7	10.1
Ethyl 2-methylbutyrate	0 – 620.4	—	—	0.07	0.4	4.7	8.5
Ethyl propionate	0 – 495.0	4.1	13.3	0.7	0.6	22.4	62.7
Ethyl butyrate	0 – 1029.6	—	—	0.4	1.3	2.5	5.4
Ethyl hexanoate	0 – 2398.0	—	—	5.6	14.9	36.2	65.5
Ethyl octanoate	0 – 3009.6	29.8	82.6	58.7	148.8	188.0	276.4
Ethyl decanoate	0 – 1039.5	—	—	34.0	75.0	82.6	119.1
Isobutanol [c]	0 – 167.8	0.1	0.5	0.1	0.3	1.1	2.5
1-Butanol [c]	0 – 62.0	—	—	—	—	0.3	0.4
Isoamyl alcohol [c]	0 – 329.7	1.5	4.27	0.20	0.59	1.2	2.9
1-Hexanol	0 – 3626.8	40.1	120.0	118.4	300.3	173.7	229.6

a) The GAM method using both monomer and dimer signals;

b) The GAM method using the dimer signal only;

c) Units for the metrics related to these compounds are mg/L.

Table 4. Correction factors to be applied to quantification results when wines of different ethanol levels are analyzed.

Compound	Calibration method [a]	Correction factor with respect to EtOH content				Equation of regression	R^2
		7%	9%	12%	15%		
Methyl acetate	Boltzmann	0.637	0.745	1.000	1.519	y = -13.56 x + 287.7	0.9848
	GAM (D)	0.625	0.735	1.000	1.563	y = -13.80 x + 280.7	0.9942
Propyl acetate	Boltzmann	0.587	0.703	1.000	1.733	y = -5.86 x + 111.9	0.9169
	GAM (M,D)	0.599	0.713	1.000	1.673	y = -5.73 x + 111.5	0.9007
	GAM (D)	0.589	0.705	1.000	1.721	y = -5.80 x + 111.2	0.9232
Isobutyl acetate	Boltzmann	0.810	0.876	1.000	1.164	y = -4.45 x + 148.0	0.9619
	GAM (M,D)	0.779	0.854	1.000	1.205	y = -4.25 x + 125.9	0.9077
	GAM (D)	0.792	0.864	1.000	1.187	y = -4.74 x + 146.9	0.9609
Isoamyl acetate	Boltzmann	0.829	0.890	1.000	1.142	y = -54.27 x + 1964	0.9469
	GAM (D)	0.849	0.904	1.000	1.120	y = -50.96 x + 2043	0.9387
Amyl acetate	Boltzmann	0.768	0.846	1.000	1.222	y = -1.31 x + 37.37	0.9323
	GAM (D)	0.751	0.834	1.000	1.248	y = -1.43 x + 38.73	0.9322
Hexyl acetate	Boltzmann	0.814	0.879	1.000	1.159	y = -24.07 x + 814.6	0.9202
	GAM (D)	0.806	0.874	1.000	1.169	y = -26.27 x + 859.6	0.9638
Ethyl butyrate	Boltzmann	0.836	0.895	1.000	1.133	y = -14.30 x + 536.8	0.9804
	GAM (D)	0.783	0.858	1.000	1.199	y = -19.76 x + 594.3	0.9830
Ethyl hexanoate	Boltzmann	0.803	0.872	1.000	1.172	y = -35.48 x + 1150	0.9432
	GAM (D)	0.786	0.860	1.000	1.195	y = -43.11 x + 1309	0.9445
Ethyl octanoate	Boltzmann	0.798	0.868	1.000	1.179	y = -102.7 x + 3261	0.9866
	GAM (M,D)	0.789	0.862	1.000	1.191	y = -109.8 x + 3370	0.9813

	GAM (D)	0.787	0.860	1.000	1.194	y = -110.7 x + 3375	0.9807
Ethyl decanoate	Boltzmann	0.837	0.896	1.000	1.132	y = -29.46 x + 1111	0.9724
	GAM (M)	0.831	0.892	1.000	1.139	y = -31.00 x + 1135	0.9764
Ethyl isobutyrate	Boltzmann	0.670	0.772	1.000	1.419	y = -23.95 x + 530.6	0.9603
	GAM (D)	0.674	0.775	1.000	1.408	y = -22.41 x + 500.8	0.9719
Ethyl isovalerate	Boltzmann	0.822	0.885	1.000	1.150	y = -2.21 x + 77.42	0.9488
	GAM (D)	0.832	0.892	1.000	1.138	y = -1.88 x + 69.05	0.9531
Ethyl 2-methylbutyrate	Boltzmann	0.824	0.886	1.000	1.147	y = -2.31 x + 81.68	0.9602
	GAM (D)	0.828	0.889	1.000	1.143	y = -2.04 x + 73.60	0.9635
Isobutanol [c]	Boltzmann	0.732	0.820	1.000	1.281	y = -0.592 x + 15.22	0.9699
	GAM (M,D)	0.795	0.866	1.000	1.182	y = -0.430 x + 13.51	0.9233
	GAM (D)	0.705	0.799	1.000	1.336	y = -0.553 x + 13.26	0.9529
1-Butanol [c]	Boltzmann	0.694	0.791	1.000	1.360	y = -0.287 x + 6.695	0.9843
1-Hexanol	Boltzmann	0.731	0.819	1.000	1.284	y = -43.89 x + 1121	0.9048
	GAM (M,D)	0.732	0.820	1.000	1.282	y = -47.62 x + 1222	0.9541
	GAM (D)	0.771	0.849	1.000	1.216	y = -39.08 x + 1128	0.9697

a) GAM (M,D) indicates the GAM method using both monomers and dimer. GAM (D) indicates the GAM method using dimers only.

Table 5. Method validation parameters of the HS-SPME-GC-MS method. Units for the calibration range, LOD, LOQ are µg/L unless otherwise indicated. For replicated trials, the standard error is displayed in the parentheses following the average value.

Compound	Calibration range	LOD	LOQ	Repeatability (n=5)	Reproducibility (n=20)	Recovery (n=12)
Isobutyl acetate	0 – 603.8	61.8	92.6	4.2% (1.0%)	5.8%	80.3% (3.4%)
Isoamyl acetate	0 – 6240.0	356.3	534.5	4.0% (0.6%)	7.3%	75.0% (1.2%)
Hexyl acetate	0 – 1627.7	118.0	177.1	5.1% (1.2%)	7.6%	67.9% (0.7%)
Ethyl butyrate	0 – 822.1	308.6	462.9	3.6% (0.4%)	6.7%	103.1% (1.2%)
Ethyl hexanoate	0 – 1540.3	74.0	111.0	4.5% (0.9%)	6.5%	40.2% (3.7%)
Ethyl octanoate	0 – 2133.7	294.4	441.6	3.6% (0.7%)	6.0%	61.9% (4.6%)
Ethyl decanoate	0 – 466.4	245.2	367.9	8.0% (2.5%)	11.2%	35.3% (4.4%)
Ethyl isobutyrate	0 – 345.3	82.9	124.4	6.0% (1.9%)	9.4%	72.2% (5.1%)
Ethyl isovalerate	0 – 66.0	5.6	8.4	3.2% (0.6%)	5.4%	20.5% (1.5%)
Ethyl 2-methylbutyrate	0 – 33.7	1.9	2.8	4.1% (0.8%)	6.5%	101.8% (0.6%)
Isobutanol [c]	0 – 155.8	24.0	36.0	6.3% (1.2%)	7.3%	101.8% (1.2%)
1-Butanol [c]	0 – 17.5	2.9	4.3	5.8% (1.0%)	7.8%	70.8% (1.0%)

Table 6. The compendium of comparison parameters between SHS-GC-IMS and HS-SPME-GC-MS methods in the analysis of wine volatile compounds, including systematic bias and the method-inherent disagreement.

Compound	Calibration method [a]	Systematic bias			Method-inherent disagreement		
		R^2	Slope	Inter-cept	Mean Difference [b]	Limits of disagreement [b]	Measurements beyond LOA [c]
Isobutyl acetate	Boltzmann	0.9108	1.26	-7.51	0.004 ± 0.71	4.3 ± 1.2	2
	GAM (D)	0.9142	2.17	-11.18	0.003 ± 0.70	4.2 ± 1.2	1
Isoamyl acetate	Boltzmann	0.9747	0.66	219.9	-0.139 ± 29.85	187.9 ± 51.7	3
	GAM (D)	0.9618	0.56	11.80	0.08 ± 36.90	232.3 ± 63.9	1
Hexyl acetate	Boltzmann	0.9912	0.97	24.82	0.013 ± 4.60	24.4 ± 8.0	1
	GAM (D)	0.9840	0.77	44.32	0.016 ± 6.22	33.1 ± 10.8	2
Ethyl butyrate	Boltzmann	0.9492	0.75	12.34	-0.004 ± 10.43	65.7 ± 18.1	0
	GAM (D)	0.9632	0.76	8.07	0.011 ± 8.81	55.5 ± 15.3	3
Ethyl hexanoate	Boltzmann	0.9736	0.97	81.32	-0.019 ± 23.71	149.3 ± 41.1	3
	GAM (D)	0.9728	1.37	-121.3	-0.022 ± 24.11	151.8 ± 41.8	1
Ethyl octanoate	Boltzmann	0.9838	1.05	59.74	0.014 ± 39.60	249.2 ± 68.6	2
	GAM (M)	0.9837	1.02	35.20	0.348 ± 39.74	250.2 ± 68.8	2
	GAM (D)	0.9831	1.00	55.21	0.083 ± 40.47	254.7 ± 70.1	2
Ethyl decanoate	Boltzmann	0.7368	1.75	260.80	-0.017 ± 29.48	156.8 ± 51.1	1
	GAM (M)	0.7381	1.78	245.00	-0.013 ± 29.38	156.3 ± 50.9	1
Ethyl isobutyrate	Boltzmann	0.7765	0.51	35.36	0.019 ± 15.95	87.6 ± 27.6	0
	GAM (D)	0.7440	0.37	46.05	0.024 ± 17.44	95.8 ± 30.2	0
Ethyl isovalerate	Boltzmann	0.9695	0.83	2.04	-0.003 ± 0.76	4.8 ± 1.3	3

	GAM (D)	0.9739	0.85	7.78	0 ± 0.70	4.4 ± 1.2	0
Ethyl 2-methylbutyrate	Boltzmann	0.9793	0.77	1.78	0.002 ± 0.58	3.6 ± 1.0	0
	GAM (D)	0.9758	0.77	6.33	-0.001 ± 0.62	3.9 ± 1.1	0
Isobutanol [d]	Boltzmann	0.8934	0.73	11.62	-0.005 ± 1.26	7.9 ± 2.2	0
	GAM (M)	0.8729	0.69	7.76	0.001 ± 1.39	8.8 ± 2.4	0
	GAM (D)	0.8934	0.72	6.64	0.001 ± 1.26	7.9 ± 2.2	0
1-Butanol [d]	Boltzmann	0.9221	0.90	0.34	0 ± 0.04	0.3 ± 0.07	0

a) GAM (M,D) indicates the GAM method using both monomers and dimer. GAM (D) indicates the GAM method using dimers only.

b) Values are expressed as average ± 95% confidence interval

c) LOA stands for the limit of agreement.

d) The units for mean difference and the limits of agreement related to these compounds are mg/L.

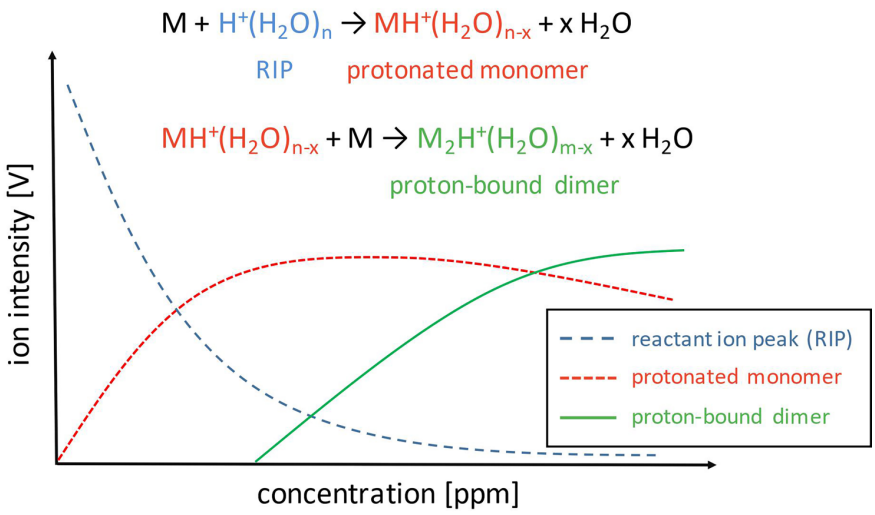

Figure 1. A schematic signal-concentration relationship curve of the monomer and dimer ions of a given compound in IMS detectors.[21] Reprinted from *Chemometrics and Intelligent Laboratory Systems*, 205, Rebecca Brendel, Sebastian Schwolow, Sascha Rohn, Philipp Weller, Comparison of PLSR, MCR-ALS and Kernel-PLSR for the quantification of allergenic fragrance compounds in complex cosmetic products based on nonlinear 2D GC-IMS data, 104128, Copyright (2020), with permission from Elsevier.

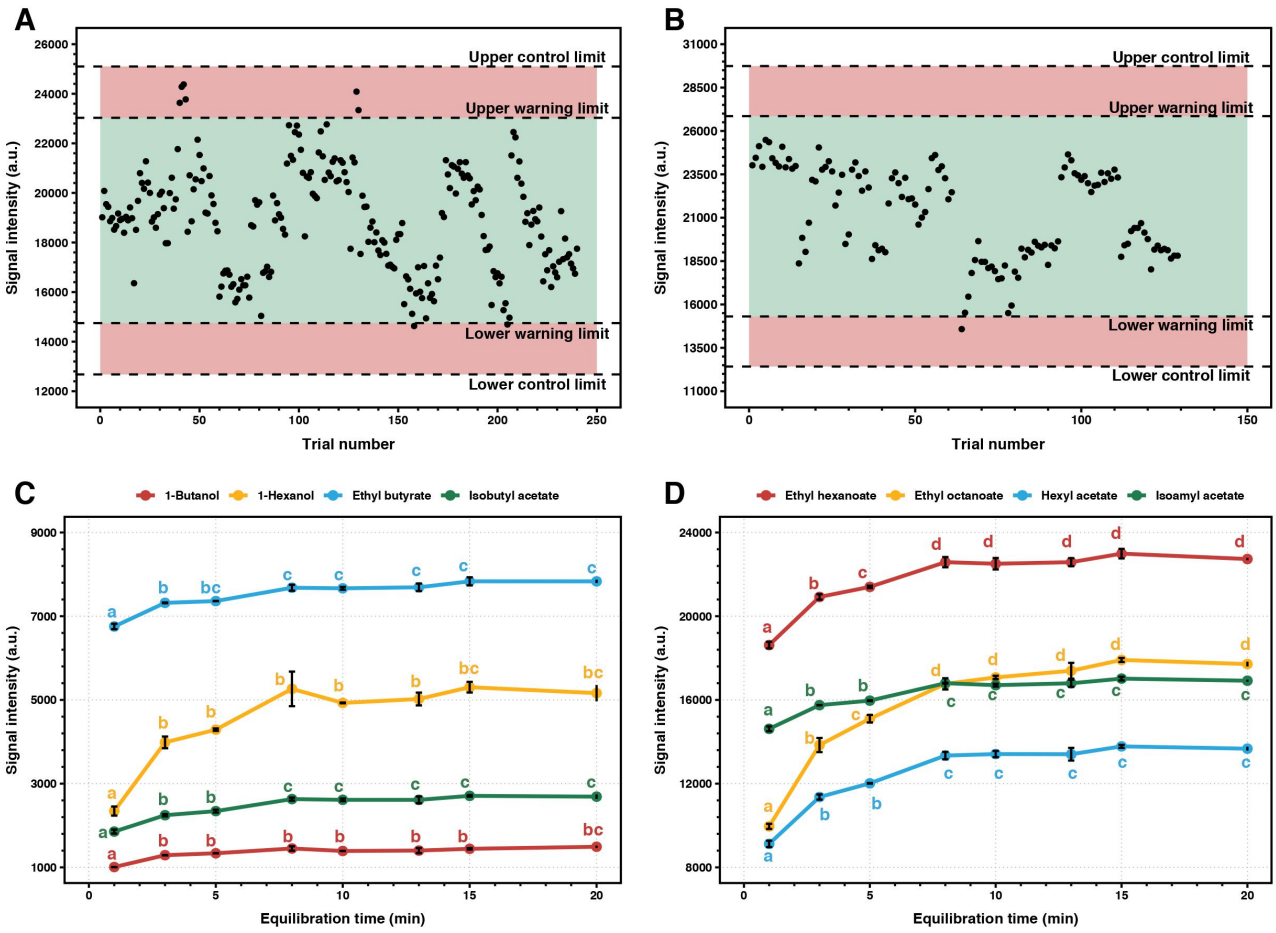

Figure 2. (A) and (B): Control charts of the first and the second batches of internal standard. Upper/lower control limit = mean value ± 3 × standard deviation. Upper/lower warning limit = mean value ± 2 × standard deviation. (C) and (D): Changes in the signal intensity of peaks of eight representative compounds in real wine samples after incubation for 2-20 minutes. Points with the different letter notations for each compound indicate statistically significant differences in signal intensities (Tukey's HSD, α=0.05).

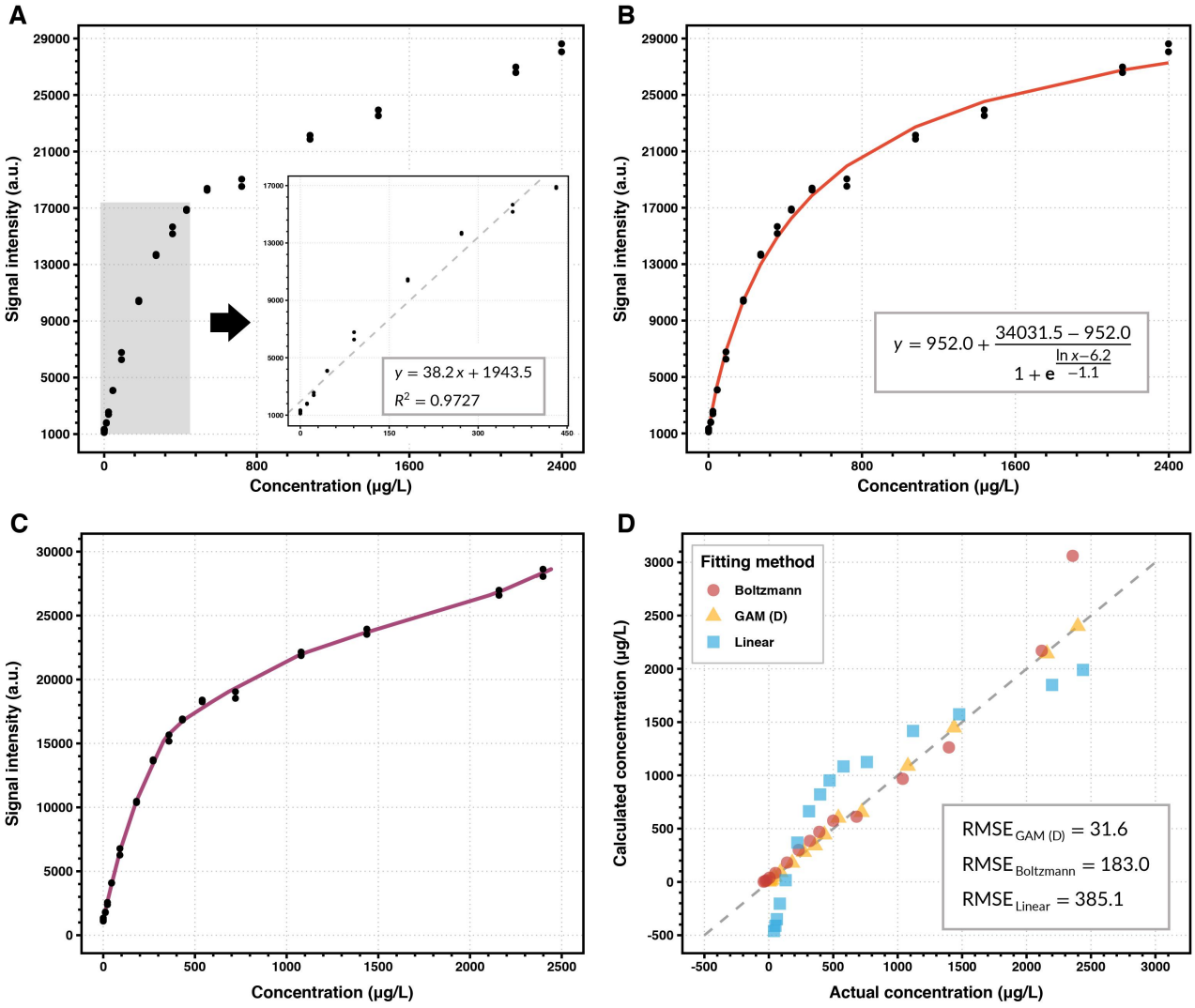

Figure 3. (A): Scatter plot of the calibration data points obtained for ethyl hexanoate in simulated wine matrix using SHS-GC-IMS. The insert shows the region where linearity is still maintained. (B): Fitting of Boltzmann function to the ethyl hexanoate calibration points with the fitted equation. In this equation, *y* represents the signal intensity (a.u.) and *x* represents the actual concentration (µg/L). (C): Fitting of GAM using b-spline functions to the ethyl hexanoate calibration points. (D): Fitting accuracy of three different methods: Boltzmann function, generalized additive model (GAM), and linear function (GAM (D) indicates dimer only used for GAM). The grey line represents the ideal model, from which increased departure intuitively indicates less reliable fitting. The goodness-of-fit is compared across different methods using root mean squared error of calibration (RMSE) as a unified metric.

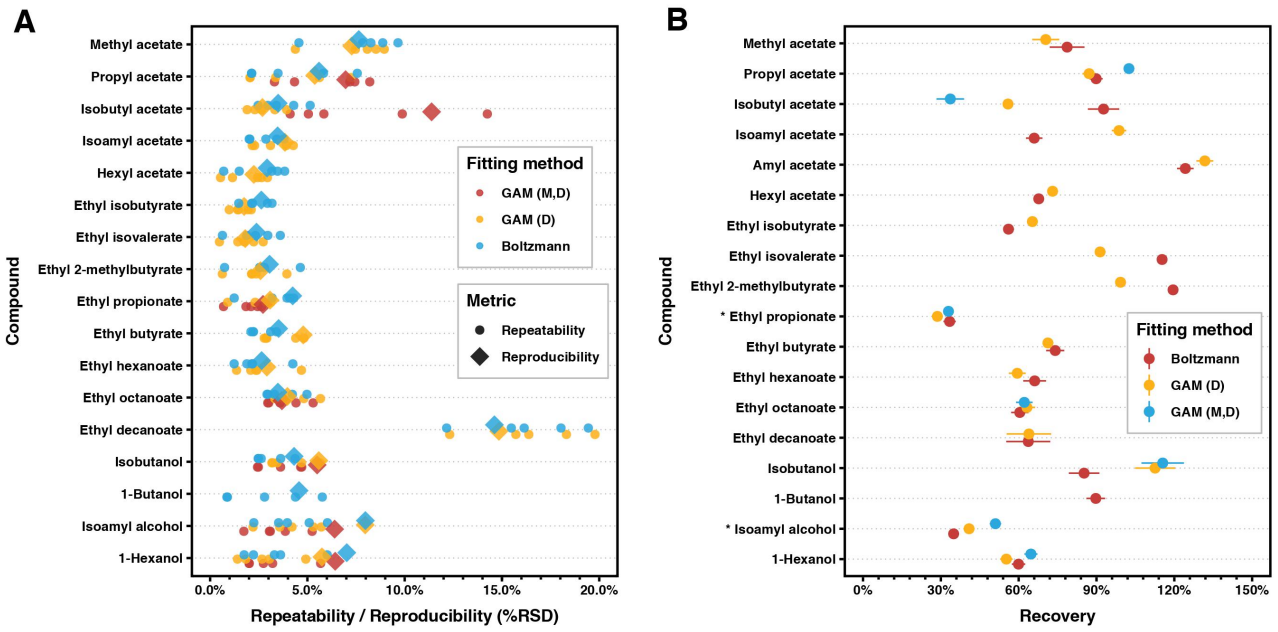

Figure 4. (A): Precision study results of the SHS-GC-IMS method with three different quantification models using real wine samples. (B): Accuracy study results of the SHS-GC-IMS method with three different quantification models using real wine samples. GAM (M,D) represents the use of both

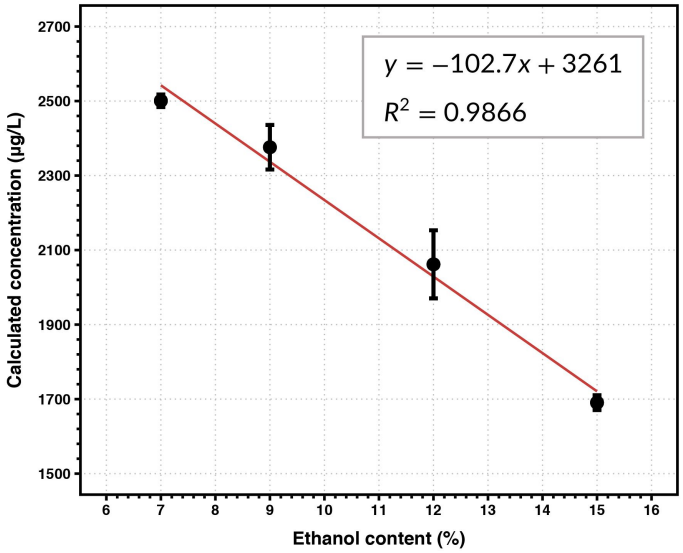

Figure 5. The ethanol content (*x*) *vs* calculated concentration of volatiles (*y*) relationship plot using ethyl octanoate as an example.

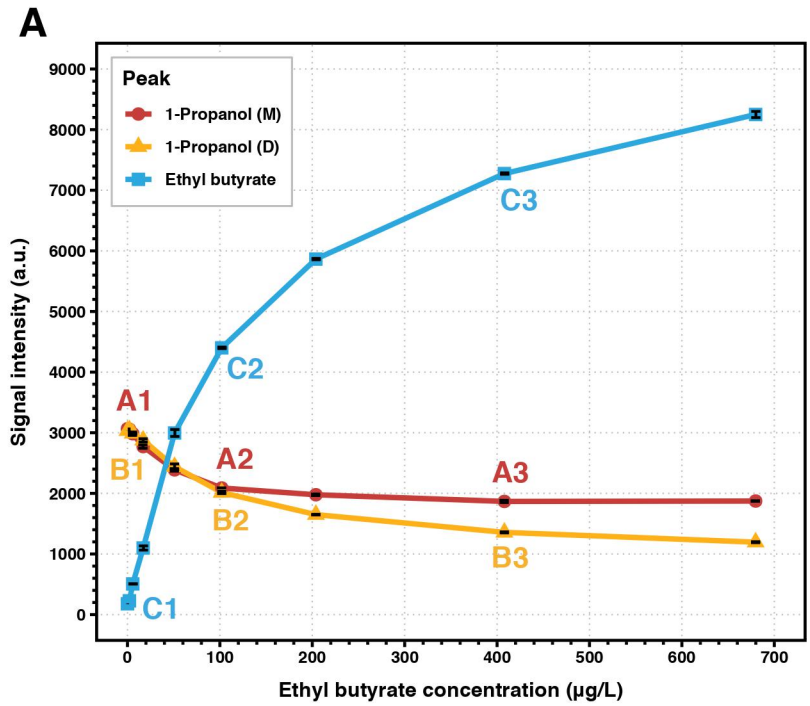
A
Peak
1-Propanol (M)
1-Propanol (D)
Ethyl butyrate
Signal intensity (a.u.)
Ethyl butyrate concentration (µg/L)
A1
B1
C1
A2
B2
C2
A3
B3
C3

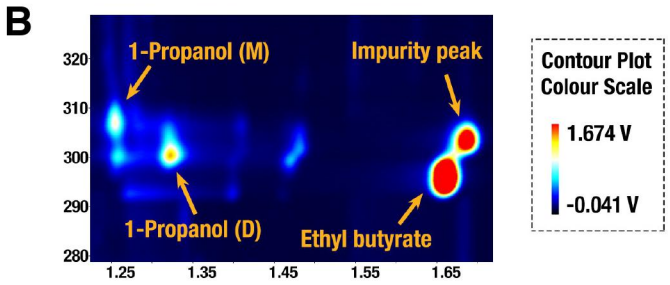
B
1-Propanol (M)
Impurity peak
1-Propanol (D)
Ethyl butyrate
Contour Plot
Colour Scale
1.674 V
-0.041 V

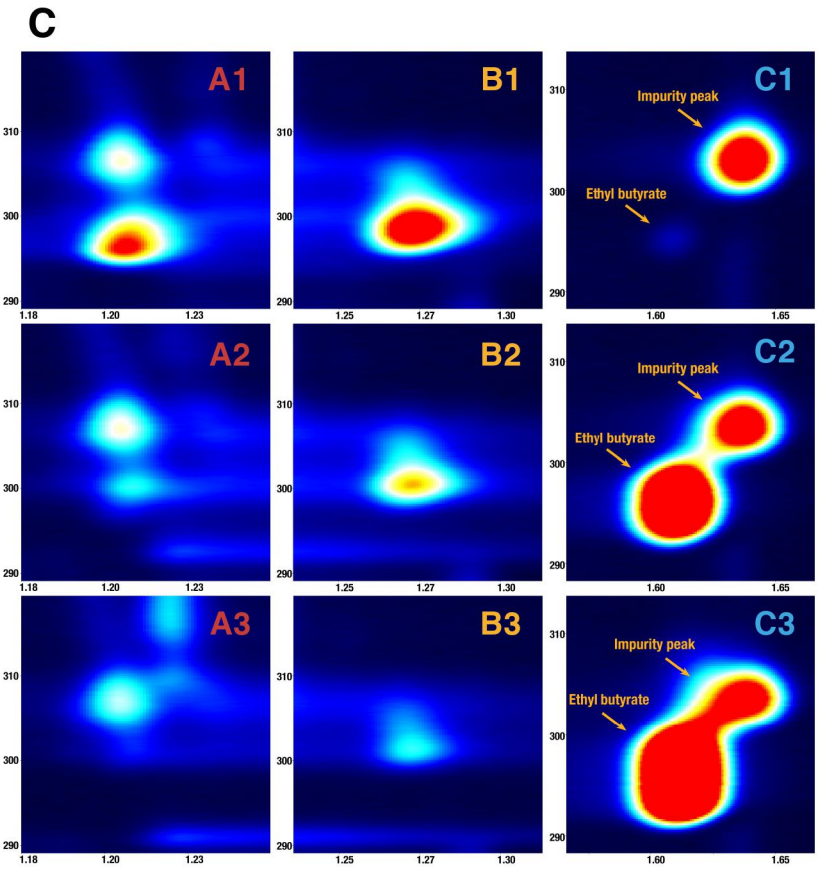
C
A1
B1
C1
Impurity peak
Ethyl butyrate
A2
B2
C2
Impurity peak
Ethyl butyrate
A3
B3
C3
Impurity peak
Ethyl butyrate

Figure 6. (A): The co-evolution curve between 1-propanol with fixed concentration of 16.3 mg/L and ethyl butyrate at 0 to 679.8 µg/L in simulated wine matrix. (B): The relative positions of 1-propanol peaks (both monomer M and dimer D) and ethyl butyrate peak. (C): Selected chromatogram snippets of 1-propanol monomer (A1, A2, A3), 1-propanol dimer (B1, B2, B3) and ethyl butyrate (C1, C2, C3). At level 1 (A1, B1, C1), ethyl butyrate concentration = 0 µg/L. At level 2 (A2, B2, C2), ethyl butyrate concentration = 51.0 µg/L. At level 3 (A3, B3, C3), ethyl butyrate concentration = 407.9 µg/L. For all chromatograms in (B) and (C), the *x* axis represents the drift time (RIP relative) and the *y* axis represents the retention time (s).

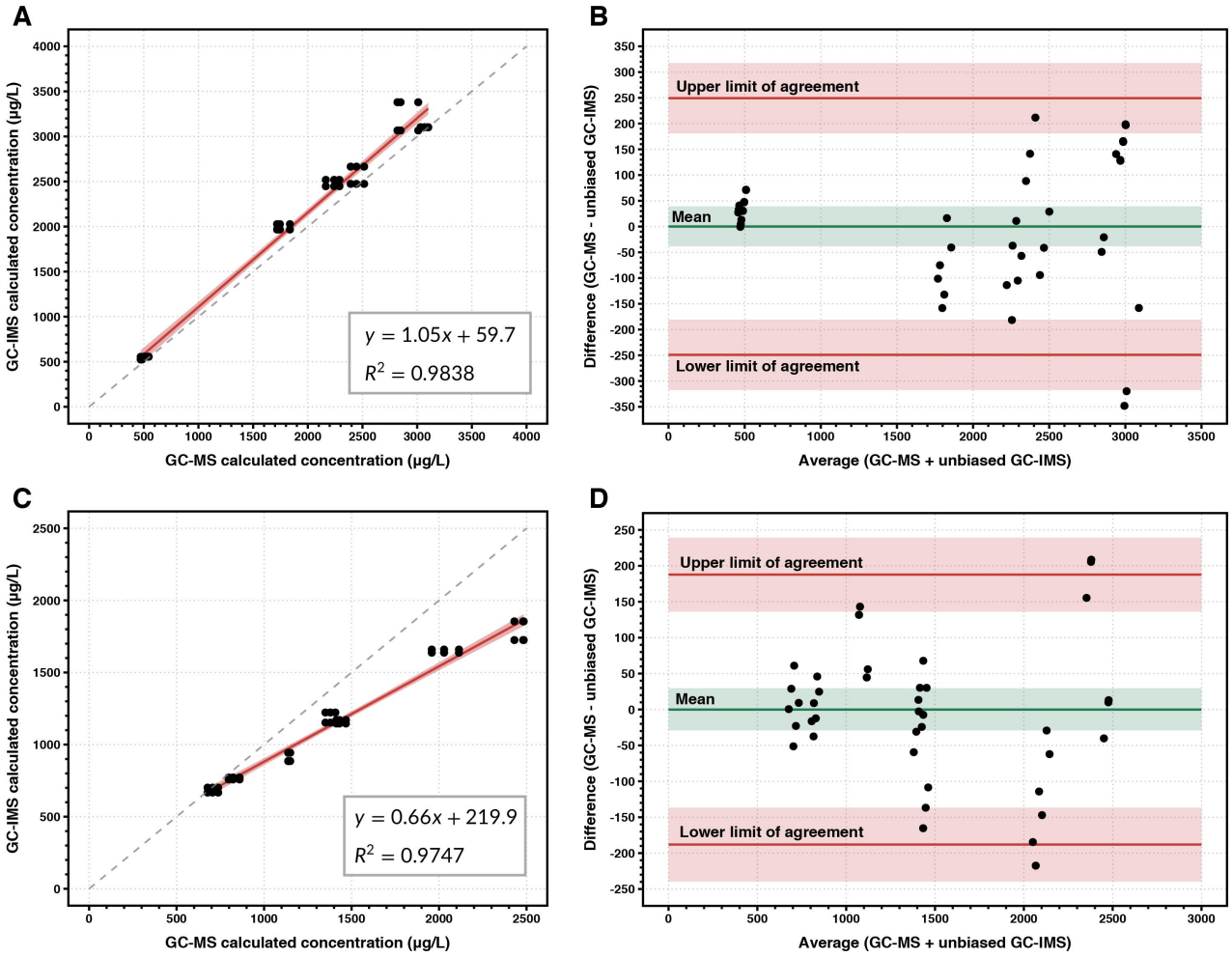

Figure 7. Correlation scatter plots between the HS-SPME-GC-MS quantification results (*x*) and the SHS-GC-IMS quantification results (*y*), as well as the corresponding Bland-Altman plots after the correction for systematic biases, exemplified using ethyl octanoate (A and B) and isoamyl acetate (C and D). For the scatter plot, the linear fitted lines are shown in red (95% confidence interval in red shade) while the ideal correlation lines (*i.e.*, *y* = *x*) are shown as grey dashed lines. For Bland-Altman plots, the average values of the limits of agreement and the mean difference are shown as red and green solid lines, respectively, whereas the shaded regions indicate their respective 95% confidence intervals.

TOC graphic

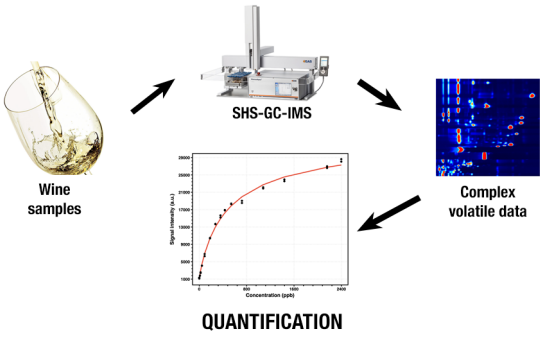
Wine
samples
SHS-GC-IMS
Complex
volatile data
QUANTIFICATION